LazyBatching: An SLA-aware Batching System for Cloud Machine Learning Inference

Yujeong Choi Yunseong Kim Minsoo Rhu
School of Electrical Engineering
KAIST
{yjchoi0606, yskimno1, mrhu}@kaist.ac.kr

arXiv:2010.13103v1 [cs.DC] 25 Oct 2020

***Abstract*—In cloud ML inference systems, batching is an essential technique to increase throughput which helps optimize total-cost-of-ownership. Prior graph batching combines the individual DNN graphs into a single one, allowing multiple inputs to be concurrently executed in parallel. We observe that the coarse-grained graph batching becomes suboptimal in effectively handling the dynamic inference request traffic, leaving significant performance left on the table. This paper proposes LazyBatching, an SLA-aware batching system that considers both scheduling and batching in the granularity of individual graph nodes, rather than the entire graph for flexible batching. We show that LazyBatching can intelligently determine the set of nodes that can be efficiently batched together, achieving an average $15\times$, $1.5\times$, and $5.5\times$ improvement than graph batching in terms of average response time, throughput, and SLA satisfaction, respectively.**

I. Introduction

As the demands for accelerating deep neural network (DNN) based machine learning (ML) algorithms increase, several hyperscalers have begun offering the compute and memory required for DNN training and inference as a service to end-users using off-the-shelf CPUs, GPUs, or custom-designed ML accelerators such as neural processing units (NPUs) [4], [28], [52]. While inference on the edge has recently received significant attention in certain application domains, major IT vendors are still predominantly deploying ML inference service over the cloud. As end-users typically desire real-time response, providing low latency inference is a fundamental requirement in cloud ML systems. However, achieving high resource utilization and system throughput is still vital in these consolidated/virtualized warehouse-scale computers as it helps optimize the total-cost-of-ownership.

Given this landscape, existing ML frameworks for *serving* ML inference requests [30], [60] provide support for *batching* inputs. Batching is an essential technique in ML frameworks to increase system throughput as it better utilizes parallelism and locality across the batched inputs. Current ML frameworks typically express the DNN algorithm as a computation *graph*, and batching is conducted in the entire graph granularity (i.e., entire DNN). These so-called *graph batching* solutions combine the individual dataflow graphs into a single one, which is concurrently executed by the backend processor in unison for higher computational efficiency and throughput [25], [60]. As all training inputs are available before the training begins, graph batching can effectively collect multiple training inputs to form a batch without any delays. However, batching inputs for inference is non-trivial as the ML inference server receives inputs at different times, the arrival rate of which is determined by the popularity of the deployed model. As such, graph batching for inference must carefully balance the tradeoff between latency and throughput. For instance, a large batch size might help improve throughput but the scheduler must then wait for a longer period of time to batch large enough inputs, suffering from an added latency. An insufficient level of batching on the other hand can help reduce latency, but comes at the cost of aggravated throughput. Consequently, existing graph batching solutions provide *model-allowed maximum batch size* (i.e., the inference server will schedule the batched input once a certain number of inputs are collected) and *batching time-window* (i.e., the longest time period the inference server will wait for inputs to form a batch) as hyperparameters of the inference server. Unfortunately, a **key challenge** of graph batching is that a statically configured batching system (with maximum batch size and batching time-window) must handle all deployment scenarios which can be suboptimal depending on the inference request traffic and available resources (Section III). For instance, having a large batching time-window is a significant overkill under lightly loaded inference request traffic because the requests queued inside the server must needlessly wait during the batching time-window, slowing down average response time. Conversely, a large batching time-window and batch size can be advantageous for periods when the server is heavily congested. The baseline graph batching however cannot flexibly adjust to the dynamic server traffic, leaving significant performance left on the table.

In this paper, we propose *LazyBatching*, an intelligent batching system that dynamically adjusts the level of batching to balance latency, throughput, and SLA (service level agreement) satisfaction. A key limitation of conventional graph batching is its inability to service newly arrived requests when an ongoing batch of requests has yet to complete its execution. Rather than having a batched input execute uninterrupted until the entire graph completes, LazyBatching maintains the scheduling granularity in fine-grained *node-level* (i.e., layer granularity) and allows different (batched) inputs to be *inter-*

This is the author preprint version of the work.

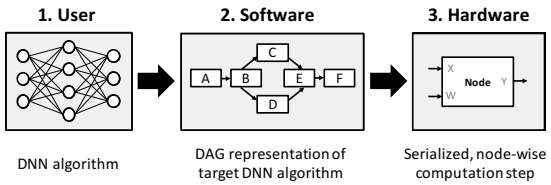

Fig. 1: DNN execution flow, from a high-level ML framework down to low-level hardware architecture.

leaved for execution. In effect, our LazyBatching scheduler can *preempt* and stall the currently ongoing batch until the newly arrived input is preferentially scheduled to *catch up* the progress of the preempted batches. Such flexible node-level scheduling enables the preempted and preempting requests to be batched at any given layer, which significantly improves the batching opportunities. Naturally, the effectiveness of "*lazily*" batching inputs as outlined above is dependent on whether the preempted batch inputs are still able to meet SLA goals despite having to wait for the newly received inputs to catch up its progress. The **key innovation** of our proposed LazyBatching is the development of an SLA-aware scheduling algorithm that utilizes domain-specific properties of ML inference to intelligently decide when/which inputs to lazily batch or not. Concretely, LazyBatching determines what is the remaining SLA *slack time* of a currently ongoing request and utilizes that information to dynamically judge whether to preempt or continue that ongoing request to satisfy SLA goals while maximizing system throughput. Because LazyBatching can flexibly adapt its batching level for both heavily or lightly loaded inference request traffic conditions, it liberates the end-user from searching the optimal batching hyperparameters (e.g., batch time-window and maximum batch size) as done in conventional, static graph batching. In effect, our proposed LazyBatching system helps improve throughput while still meeting the SLA goals of cloud ML inference. Below we summarize our **key contributions**:

- We develop an SLA-aware slack prediction model which exploits a domain-specific property of ML inference to predict the DNN inference time for slack estimation.
- We propose LazyBatching, a low-cost and practical batching system for cloud inference. Unlike prior work, our solution is not limited to a particular type of a DNN layer and can flexibly adapt to the deployment environment without hand-tuning the batching parameters.
- Compared to graph batching, LazyBatching provides an average $15\times$, $1.5\times$, and $5.5\times$ improvement in latency, throughput, and SLA satisfaction, respectively.

II. Background

A. Deep Neural Networks

Deep neural network (DNN) based ML applications are represented as a direct acyclic graph (DAG) in popular ML frameworks [9], [21], [26]. Each node within the DAG corresponds to a DNN layer, which is commonly designed using convolutional, activation, pooling, fully-connected, and recurrent layers. Figure 1 shows how the DAG based DNN

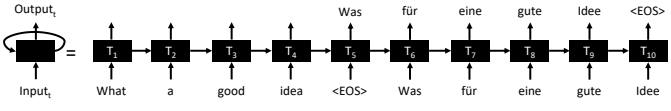

Fig. 2: A *vanilla* recurrent layer unrolled into ten sequence length in this English-to-German translation example. For different input sentences, the output sequence length can be different (e.g., "The sky is blue"→"Der Himmel ist blau"). The recursive, time-unrolling effects in attention-based NLPs [17], [64], [79] are observed in the decoder blocks of these algorithms.

is lowered into a serialized, node-wise (i.e., layer-wise) execution step. ML applications for computer vision are primarily based on convolutional neural networks (CNNs) using convolutional and fully-connected layers. These DNN applications typically have a *static* graph topology where the number of nodes within the graph and its structure are fixed (e.g., the DAG in Figure 1). In contrast, DNNs used for speech recognition [5] or natural language processing (NLP) [17] exhibit a *dynamic* graph structure in that they have *variable* number of graph nodes to traverse within the DAG. These applications are designed to model the so-called "sequence-to-sequence" (seq2seq) behavior: e.g., translating a English sentence to German involves mapping a variable length sequence of English words into a variable length sequence of German words [78]. As such, the DNNs used to model the seq2seq behavior have *recursive* computations, rendering the graph topology of these DNNs to be dynamically derived in an input-dependent manner. In other words, the recursive computations within these dynamic graphs must be *unrolled* in order to accurately reflect the seq2seq behavior (Figure 2). Seq2seq models traditionally utilized recurrent neural networks (RNNs) using LSTM or GRU cells as building blocks for the recurrent layers [15], [34]. Recent work however demonstrated that *attention* modules (pioneered by the work on *Transformers* [79]) can achieve superior algorithmic performance than RNNs (e.g., BERT [17], GPT-2 [64]). Consequently, state-of-the-art NLP applications are primarily designed using attentions these days.

B. Batching for Training vs. Inference

A DNN application must be *trained* in order to be deployed for *inference*. Batching is a critical component for both training and inference in today's ML frameworks as it helps increase throughput and optimize the total-cost-of-ownership in cloud ML systems. Because the training dataset is already available before the learning process begins, constructing a large enough batch size is trivial for training. However, collecting batched inputs for inference is challenging because the server receives DNN inference requests at varying rates, which is determined as a function of how popular the deployed model is, what time of the day the requests are being received, and etc. In the rest of this paper, we focus on inference which has unique challenges in developing an effective batching system.

C. Batching on Latency vs. Throughput

Popular ML model serving frameworks such as TensorRT Inference Server [60] or TensorFlow Serving [30] conduct

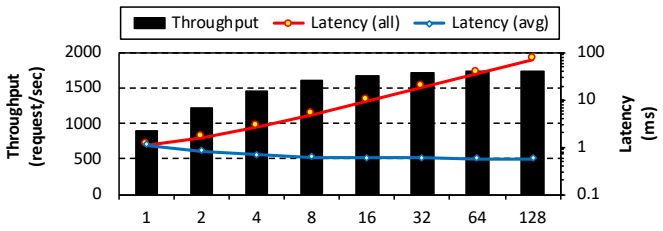

Fig. 3: Effect of batching on throughput (left-axis) and overall latency of batched execution (red, right-axis) as a function of batch size (x-axis). To show the benefits of batched execution on reducing the average latency per each individual input, the blue line represents average latency per each input (i.e., Latency(all)/number of batches) on the right-axis. For this experiment, we assume that the batched inputs are already formed at size N, without waiting for them to be collected.

batching in the entire *graph* granularity. These so-called *graph batching* solutions combine multiple individual DAG into a single, batched DAG, allowing the backend processor to execute them in parallel. Figure 3 shows the effect of graph-level batching in ResNet's effective throughput and latency. As depicted, the effective throughput rapidly increases as batch size gets larger, which amortizes the cost of inference and translates into a sharp reduction in average inference latency per each input (the blue line, Latency(avg)). This is because having a larger batch size increases the required computations which helps better saturate the abundant computing resources within GPUs/NPUs for higher throughput. However, the increase (decrease) in throughput (latency(avg)) eventually levels out beyond a certain batch level, highlighting the importance of selecting an optimal level of batching that balances throughput and latency.

D. Research Scope

While throughput-optimized GPUs fit well for training, they are often deemed ill-suited for latency-critical, low-batched inference because of their low utilization [33], [40]. Consequently, recent cloud ML systems [23], [36], [40], [53], [84] employ custom designed NPUs for deployment (e.g., Google's TPU [27], Habana's Goya [31], Facebook's Kings Canyon [22]). LazyBatching is applicable for both GPUs and NPUs, but given the popularity of NPUs for latency-critical inference scenarios, we assume NPUs as the baseline accelerator architecture in this paper. Nonetheless, LazyBatching's effectiveness over GPU-based inference systems is quantitatively demonstrated in Section VI-C.

III. Motivation

A. Limits of "One-Size-Fits-All" Batching

Conventional graph batching takes a "one-size-fits-all" approach, which utilizes the following two hyperparameters to optimize the ML inference server. First, the *model-allowed maximum batch size* is used to configure the scheduler to only batch inputs up to the point where having a larger batch size helps improve throughput while still improving user-responsiveness. In Figure 3 for instance, it is practically meaningless for the ML inference server to batch inputs beyond 16 for ResNet as the effective throughput is saturated

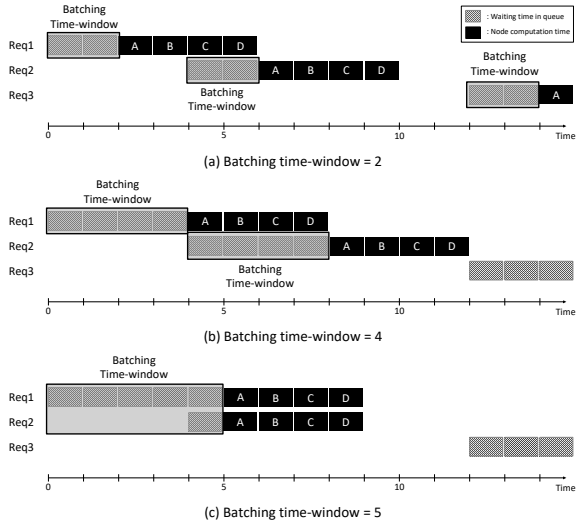

Fig. 4: Timeline of baseline graph batching when the batching time-window is changed. Example assumes the server receives $Req2$ and $Req3$ at t=4 and t=12, respectively.

beyond this point. Second, the ML inference server is also setup with a *batching time-window* which is the maximum period of time the scheduler waits for incoming requests to form a larger batch. When the request traffic to the inference server is lightly loaded, having a smaller batching time-window prevents the server from needlessly waiting for future inputs to batch. For instance, increasing batching time-window from 2 to 4 in Figure 4(a-b) does not help increase batch size and needlessly delay the time $Req1$ and $Req2$ can start execution. Conversely, when the inference request traffic is high, this hyperparameter can help guarantee that the server waits long enough to form a larger batch to increase throughput while not harming latency (Figure 4(b-c)). Notice how the optimal batching time-window and model-allowed maximum batch size is determined as a function of what the request traffic to the inference server is, what the throughput-vs-latency tradeoff curve is for a given processor architecture (Figure 3), and others.

Overall, a fundamental challenge of graph batching is that the *statically* chosen batching time-window and maximum batch size is utilized to handle *all* scenarios, even though it is practically impossible to estimate when the candidate inputs for batching will arrive at the ML inference server. When the server is lightly loaded, it is better to optimize the inference server for latency with a short batching time-window with low maximum batch size. Conversely under heavy request traffic, optimizing the inference server for both latency and throughput with a large enough batching time-window is preferrable (Figure 5). Unfortunately, the baseline (static) graph batching by design cannot adapt to the dynamic request traffic patterns. Consider a scenario where the scheduler just issued a new batched input prematurely (i.e., increasing batch size further helps improve throughput while having minimal impact on latency) for execution because the batching time-window elapsed (Figure 4(b)). If the server receives new inputs just after such batched input was scheduled, a better

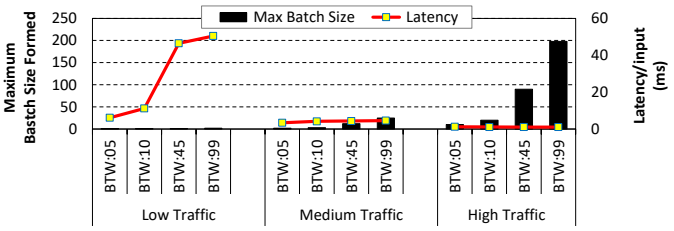

Fig. 5: Effect of batching time-window (BTW, from 5 ms to 99 ms) on baseline graph batching's maximally formed batched size (left-axis) and average latency per input (right-axis) for ResNet, as a function of input request traffic load (x-axis). For low traffic conditions, a larger batching time-window does not help improve throughput and only end up harming average latency per input. Under heavy traffic, batching inputs starts being effective in improving throughput while still help reduce average latency per each input. This figure assumes 16/250/2000 requests/sec query-arrival rate to model low/medium/high traffic. Section V details our methodology.

scheduling decision would have been to wait a bit longer (i.e., larger batching time-window) and seek a larger batch size (Figure 4(c)). The static, "one-size-fits-all" approach of graph batching however is not able to properly handle the aforementioned scenarios and reduce batching opportunities.

B. Pitfalls of "Application-Specific" Batching

To tackle the limitations of graph batching, recent work by Gao et al. [25] proposed *cellular batching*, which partially addresses the batching problem from an application-specific perspective, with an emphasis on RNN inference. A distinguishing feature of RNNs is that the RNN cells within the time-unrolled recurrent layers all share the same weight values across different timesteps (Figure 6). Cellular batching utilizes such property to batch at the level of RNN cells rather than the entire DAG, allowing new input requests to be batched into an ongoing batched request. Figure 6 shows the different batching behavior between graph vs. cellular batching. The baseline graph batching assumes that the first 2 requests (Req1-2) form a batch and starts execution at the beginning of time. As the initial batched execution does not get completed until t=5, the newly arrived requests (Req3-5) remain idle inside the server, waiting for the current batch to finish execution. Cellular batching can immediately schedule Req3 for execution as it can be batched with Req1-2 at t=1 (and similarly, Req4 at t=4). This is possible because the unrolled RNN cells all share the same weight parameters across different timesteps (e.g., Req3-4 and Req5 all execute using the same weights at t=5), enabling the batching system to more flexibly merge requests at a fine-grained cell level. Overall, the benefit of cellular batching is as follows. First, cellular batching can reduce average response time as the newly arrived requests can immediately join ongoing batched requests without having to wait during the batching time-window. Second, it also helps improve system throughput as the likelihood of batching is significantly improved thanks to the fine-grained, cell-level batching. However, a key challenge of cellular batching is its limited applicability among generic DNN workloads. Because cellular batching is specifically designed to leverage the unique feature of RNNs (i.e., unrolled

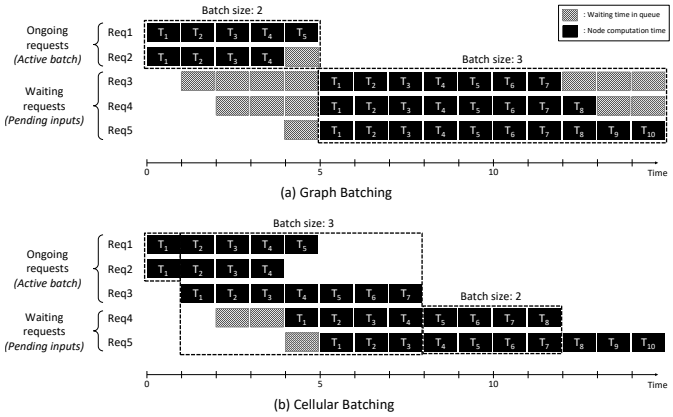

Fig. 6: Timeline of (a) graph batching and (b) cellular batching when three requests (Req3 to Req5) are received while Req1-2 are being processed. Figure assumes that each request is executing an RNN, each with a different output sequence length (determined by the number of times the recurrent layer is time-unrolled, e.g., Req1 with 5 timesteps while Req5 with 10 timesteps). The model-allowed maximum batch size is assumed to be configured to 3, which delays Req4 from being batched until t=4.

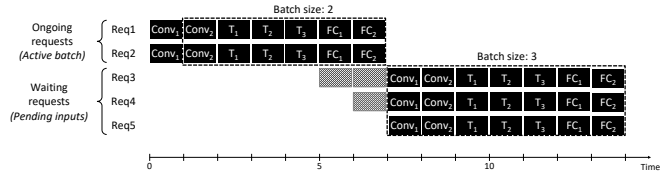

Fig. 7: An example scenario where cellular batching fails to batch inputs (e.g., DeepSpeech-2). DNN graph is assumed to have two convolutional ($\texttt{CONV}_i$) and two fully-connected layers ($\texttt{FC}_i$) before/after the recurrent layer.

recurrent cells share the same parameters), the weight sharing effect it takes advantage of is no longer applicable when the end-to-end DNN application contains *non*-RNN layers (e.g., convolutional or fully-connected layers). Consider the example shown in Figure 7 which provides a high-level overview of DeepSpeech-2's execution timeline using cellular batching. Once the first batch Req1-2 starts execution, cellular batching is not able to batch the newly requested inputs Req3-5 into the ongoing batch. This is because the future inputs Req3-5 must start executing from the first convolutional layer yet the ongoing batch is already further down the execution process. As such, cellular batching effectively levels down into the baseline graph batching, *serializing* the scheduling of Req1-2 and Req3-5 for DNNs containing non-RNN layers within.

C. Our Goal: A Flexible and Robust Batching System for ML

Overall, we observe several challenges with prior batching architectures. First, baseline graph batching applies a brute-force, static solution to all deployment scenarios which is suboptimal in handling the dynamic inference request traffic patterns. Second, an application-specific batching solution like cellular batching is optimized for a unique property of a specific (RNN) layer, so it can be inapplicable for newly developed DNN layers or complex topologies (Figure 7). Given how fast evolving the ML algorithmic research space has been recently (e.g., state-of-the-art ML algorithms for NLP are no

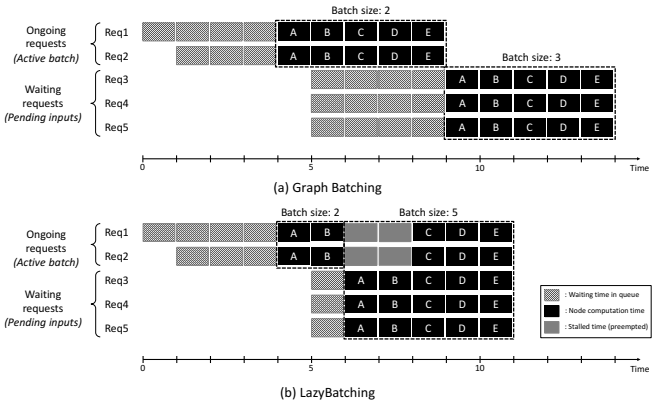

Fig. 8: Proposed LazyBatching execution timeline (vs. baseline). Each DNN is assumed to contain a fixed size of five graph nodes (node A to E).

longer powered by RNNs but rather designed using attention modules [17], [64]), a batching system tailored for a subset of the DNN algorithms is unlikely to remain effective for the constantly evolving ML research space. Lastly, it is of vital importance for end-users purchasing MLaaS to minimize SLA violations while maximizing throughput for cost-efficiency. As we demonstrate in Section VI, our SLA-aware batching can seamlessly adapt to the dynamic traffic patterns, achieving low latency while improving system throughput at all times. Such property not only helps hyperscalars seeking to optimize TCO but also the end users of MLaaS. This is because low-latency and high-throughput can be achieved simultaneously, without having to painstakingly fine-tune batching time-window, maximum batch size, or other design parameters of graph batching, causing less burden to MLaaS consumers.

Our goal is to develop a batching system that can flexibly adapt to the dynamically changing inference request traffic while also being widely applicable for both current and future DNN topologies. In the following section, we detail our proposed batching architecture which fundamentally addresses the limitations of prior batching solutions.

IV. LazyBatching: SLA-Aware Batching System for Cloud Machine Learning Inference

We propose LazyBatching, an intelligent batching system that can dynamically adapt its batching granularity to balance latency, throughput, and SLA satisfaction.

A. Proposed Approach

While the end-to-end DNN application is represented as a graph structure, the execution itself is conducted in a fine-grained *node* (or layer) granularity by the backend processor. Concretely, the runtime system in a typical ML framework (e.g., TensorFlow, PyTorch, Caffe2) determines the sequential order the graph nodes are to be executed for a target DNN model, and schedules each individual nodes to the processing unit for execution (Figure 1). As a result, user-level runtime APIs in popular backend DNN libraries such as NVIDIA's cuDNN [59] are designed in accordance to such node-level execution model (e.g., `cudnnConvolutionForward()`).

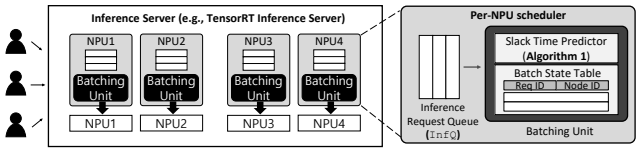

Fig. 9: High-level overview of LazyBatching model serving system.

Conventional batching systems however are based on a coarse-grained, *graph-wide* scheduling framework, which is at odds with the *node-level* DNN execution model. As highlighted in previous sections, a key limitation of graph batching comes from its rigid, static graph-wide scheduling. Concretely, once a batched graph is scheduled for execution, future inputs cannot execute until the currently ongoing batch is finished. Such constraint poses a fundamental challenge in the batching opportunities between an ongoing batch and a newly requested input because they cannot share a common layer (i.e., graph node) to execute simultaneously.

Rather than having a single batched input exclusively execute until completion, our **key approach** is to maintain the scheduling granularity in a fine-grained *node-level* and allow different (batched) inputs to be *interleaved* for execution. LazyBatching utilizes the node-level scheduling framework to preferentially schedule newly requested inputs to *catch up* the progress of a previously ongoing, but yet to be finished earlier inputs. This opens up more batching opportunities as inputs can be *"lazily"* batched with each other in an incremental manner. The notion of batching time-window is therefore non-existent with LazyBatching because there is no fixed-length time window which inputs must wait in order to be batched together. In effect, our LazyBatching scheduler constantly fires off one of the nodes within the pool of schedulable inputs, whenever the batching unit finds that appropriate to meet latency, throughput, and SLA goals. Figure 8 illustrates an example where our scheduler virtually *preempts* the execution of batched inputs Req1-2 at t=6 and *context switch* to the execution of Req3-5 until it catches up the progress Req1-2 has made before it was preempted. Once the context switched Req3-5 executes up to node B at t=8, both Req1-2 and Req3-5 now share a common layer which our scheduler can safely *merge* as a single batch to resume execution starting with node C. Note that the preemption of an ongoing batch, followed by a context switch to another (potentially batched) input, is *always conducted in layer boundaries* by the runtime system at user-level because LazyBatching naturally exploits the node-level scheduling framework (i.e., an ongoing batch will never get interrupted until its *intra-node* computations are finalized). In other words, the node-level preemption and context-switching *does not require any hardware modifications* and is *done purely in software* using existing ML frameworks and runtimes (Section VI-D details the implementation overhead).

Nonetheless, the effectiveness of lazily batching requests is dependent on whether the fine-grained interleaving of different input requests does not harm the responsiveness of individual inputs or violate SLA goals. A **key innovation** of

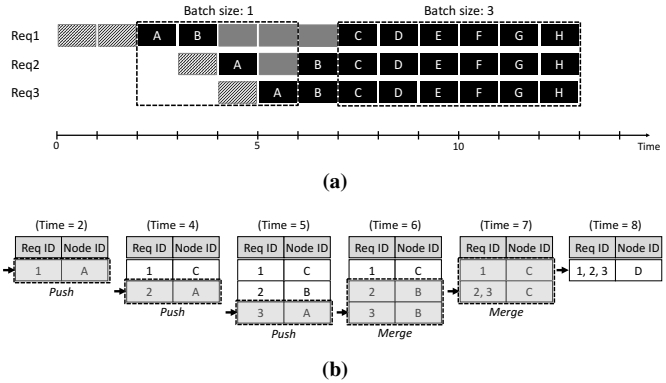

Fig. 10: (a) Timeline of LazyBatching when executing a graph with 8 nodes, and (b) the changes in `BatchTable` as stack entries are *pushed/merged*. Example assumes that the slack time predictor always find lazily batching pending input requests (Req2-3) with the active batch (Req1) beneficial. The stack grows from top to bottom in this figure (i.e., the black arrow points to the top of the stack).

LazyBatching is the development of an *SLA-aware, slack time prediction model* which our scheduler utilizes to intelligently judge when/which inputs are worth lazily batching. In the rest of this section, we first detail our model serving architecture followed by our slack time prediction model.

B. LazyBatching Model Serving Architecture

Figure 9 provides a high-level overview of LazyBatching's model serving system. When the ML inference server receives an inference request, it is first forwarded to the inference request queue (`InfQ`) and waits until the scheduler issues it (either in isolation or as a batch, grouped with other inputs) to the backend processor. There are two key components that constitute our LazyBatching server system. First, our batching system maintains a *batch state table* (`BatchTable`) that tracks the batching status among the inputs currently executing. Second, an *SLA-aware slack time predictor* is employed which utilizes domain-specific properties of ML inference to analyze whether lazily batching the currently executing inputs and the ones waiting in the `InfQ` (henceforth referred to as *active batch* and *pending inputs*, respectively) will result in an SLA violation or not.

When the SLA-aware slack time predictor determines that an additional batching can violate SLA, then the scheduler does not try to batch more inputs and authorize the currently active batch to complete its execution uninterrupted. However, if the likelihood of an SLA violation through lazily batching is low, then our scheduler first preempts the active batch at the end of the current node. It then context switches to the pending inputs to allow it to catch up the progress of the preempted, previously active batch. During the course of this process, the `BatchTable` keeps track of the layer-wise execution status of the preempted and preempting inputs so that they can be batched together once they reach the same graph node. Below we first discuss how LazyBatching utilizes the `BatchTable` for node-level scheduling and batching.

Stack-based batch status tracking. LazyBatching implements the `BatchTable` as a software *stack* data structure and the entry at the top of the stack corresponds to the active batch that is currently executing. Each stack entry tracks what is the graph node ID a group of batched inputs (referred to as *sub-batch*) will be executing. LazyBatching utilizes the `BatchTable` to examine a sub-batch's basic requirements to be batched with other sub-batches (i.e., whether they are able to execute a common node). Figure 10 shows how the `BatchTable` is utilized to lazily batch incoming requests on-the-fly. Because the `InfQ` only has a single input $Req1$ initially, the top of the stack entry (one corresponding to this sub-batch) is *pushed* with a request ID of 1 and node ID A as shown in t=2 of Figure 10(b). Suppose the inference server receives another input $Req2$ while $Req1$ is busy executing node B, and the SLA slack predictor deems it advantageous to merge $Req1$ and $Req2$ as a single batch. In situations like this, our scheduler first updates the next graph node ID of our active batch $Req1$ to node C at the end of node B's execution to designate the fact that this sub-batch should execute node C once the scheduler issues it again to the processor. The scheduler then preempts the execution of $Req1$ and pushes another stack entry corresponding to $Req2$ (i.e., request ID of 2 executing node A) to the `BatchTable` so that $Req2$ becomes the *new* active batch to be issued to the processor (at t=4 of Figure 10(b)). As the scheduler context switches to $Req2$ and executes node A, the server receives another request $Req3$, which the slack predictor decides to lazily batch it with $Req1$-2. This is done by again preempting $Req2$ at t=5 when it finishes executing node A, and then pushing another stack entry of $Req3$ to have the scheduler execute $Req3$ afterwards. Once the new active batch $Req3$ finishes executing up to node A, the node ID field in the stack is updated to B (t=6 at Figure 10(b)). Notice how the node ID field of the two topmost stack entries are now identically at node B, meaning all the inputs that are part of these two sub-batches can be merged as a single batch. The batching of these two entries is undertaken by *merging* the two topmost stack entries as a single one, as illustrated in t=6 of Figure 10(b), which allows both $Req2$ and $Req3$ to execute concurrently starting graph node B. Figure 10(b) similarly shows the updates to the `BatchTable` when the batched $Req2$-3 gets lazily batched again with $Req1$ at t=7. Because the stack push/merge operations are only invoked at layer-boundaries in software, `BatchTable` enables a low-cost yet high performance control mechanism to track batching status.

C. "SLA-Aware" Slack Time Prediction

Providing fast user responsiveness is of utmost importance for user-facing ML inference, so cloud service providers typically have SLA targets to meet to satisfy QoS requirements. LazyBatching utilizes our *SLA-aware slack time prediction* model to only authorize batching when it will not violate the SLA. Our prediction model quantifies how much slack time a given batched input has remaining before violating a model-specific SLA target. The estimation of a batched input's slack time is done conservatively (i.e., predict that SLA slack time is smaller than what actually remains) such that the scheduler is optimized to minimize the number of SLA violations first

Algorithm 1 DNN graph-wide inference time estimation

```
1:  SingleInputExecTime ← 0
2:  GraphLatency ← 0
3:  for n in nodes do
4:      if Type(n) is STATIC then
5:          GraphLatency += NodeLatency(n)
6:      else if Type(n) is ENCODER then
7:          GraphLatency += NodeLatency(n) × enc_timesteps
8:      else
9:          GraphLatency += NodeLatency(n) × dec_timesteps
10:     end if
11: end for
12: SingleInputExecTime ← GraphLatency
13:
14: return SingleInputExecTime
```

and improve throughput second. Our SLA-aware slack time estimator consists of three key components: 1) node-level latency estimation, 2) graph-wide estimation, and 3) utilizing these two components for slack estimation. We first detail our definition of SLA slack time, followed by a description of our node-level/graph-wide latency estimation model.

Slack time prediction. Consider the first request $Req1$ in Figure 10, which we use as a running example to explain our slack model. If the processor is currently busy handling other requests, $Req1$ will have to wait in `InfQ` until it gets issued to the processor for the first time (two time-units, from t=0 to 2 in Figure 10(a)). Because the initial server wait time (T_{wait}) also counts against SLA, our model needs to subtract T_{wait} from the model-specific, constant SLA value (SLA_{target}) when estimating slack. Once $Req1$ starts execution, $Req1$'s remaining slack becomes a function of how long it will take for $Req1$ to complete the end-to-end DNN execution. Accordingly, the slack time of $Req1$ *without* batching is:

$$Slack = SLA_{target} - (T_{wait} + SingleInputExecTime_{Req1}) \quad (1)$$

For an SLA_{target} of 30 time-units, then the slack time without batching is estimated as "30−(2+8)=20" for the given examples in Figure 10 (i.e., 8 time-units is consumed when $Req1$ executes node A to H). However, under a scenario where $Req1$ *is* batched with $Req2$, the *SingleInputExecTime* term in Equation 1 should incorporate the batching effects for slack estimation. If we were to have the exact throughput-vs-latency tradeoff curves for every graph node within the target DNN model (similar to Figure 3, but evaluated for every graph node under all possible inference batch size), we can quantify the impact the potential (lazy) batching between an active batch ($Req1$) and pending inputs ($Req2$) will have on end-to-end inference latency. Maintaining such *oracular* tradeoff curve for all possible graph nodes and batch size however is cumbersome let alone requires a high implementation overhead. As the primary goal of our slack estimation is to minimize SLA violations, we propose to *conservatively* estimate the inference latency of *batched* inputs as a summation of all input's *single-batch latency, executed in isolation*. While this *overprovisions* the estimated inference time of *batched* inputs, it helps reduce the estimated slack time thereby reducing the likelihood of SLA violations.

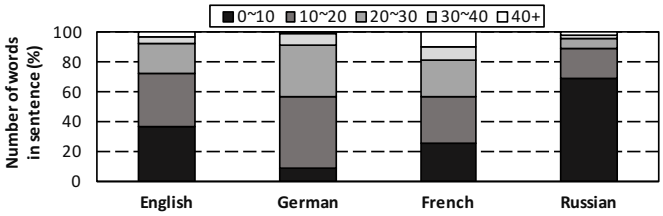

Fig. 11: Number of words within a sentence when characterized across WMT-2019's 30,000 "English-to-German/French/Russian" translation pairs [83].

Equation 2 summarizes our slack time prediction model which assume the initial input ($Req1$) is batched with $(N-1)$ future requests:

$$Slack = SLA_{target} - (T_{wait} + \sum_{i=1}^{N} SingleInputExecTime_i) \quad (2)$$

In Section VI, we quantitatively demonstrate that our conservative slack estimation model is competitive even compared to its *oracular* version, which utilizes the aforementioned oracular tradeoff curve in estimating a batch's precise execution time. As both SLA_{target} and T_{wait} are known values, deriving the $Slack$ value in Equation 2 requires an estimation of an individual, single-batched input's end-to-end, graph-wide execution time (i.e., $SingleInputExecTime_i$). We now discuss our node-level/graph-wide latency estimation model for predicting $SingleInputExecTime_i$ (Algorithm 1).

Node-level latency estimation. Our key observation is that each individual graph node's execution time over a target hardware architecture is highly deterministic and predictable. A graph node's layer configuration is determined at compile time and the layer weight values are also statically fixed for inference. As a result, the computation and memory access characteristics of a graph node (i.e., DNN layer) is highly regular and input-independent, exhibiting little per-layer latency variation across different executions. Prior work [20], [39] similarly observed the deterministic nature of DNN inference and our node-level latency estimator exploits such property. We therefore propose to *profile* the per-node execution time of the target DNN and characterize its average per-node latency as a software-level lookup table. The node-level latency lookup table ($NodeLatency(n)$ in Algorithm 1) is then utilized for estimating the DNN's graph-wide execution time. The profiling overhead is negligible as the characterization of a DNN graph's node-level latency only has to be done once and be reused for all future inferences for that model.

Graph-wide latency estimation. Predicting the graph-wide execution time requires an estimation of how *many* graph nodes to traverse for a given DNN's inference. As discussed in Section II-A, DNNs with a *static* graph topology have a fixed number of nodes to execute, irrespective of what the input value is. Consequently, estimating the graph-wide inference time of a static DNN (e.g., CNNs) is straighforward where we simply conduct a summation of all the node-level latency estimations as summarized in line 3-5 of Algorithm 1.

However, precisely estimating the latency of a *dynamic* graph DNN is challenging, if not impossible, because the number of nodes to traverse within the DAG is variable and input-dependent. Consider the English-to-German translation example shown in Figure 2. Depending on what the input (English) sequence length is, the output (German) sequence length can vary, represented by the number of times the recurrent layer in RNNs (or the decoder block in attention modules [17], [79]) have been time-unrolled. Because the number of unrolled timesteps (i.e., the number of translated German words) is determined dynamically at runtime, statically estimating the graph-wide inference time is challenging.

Nonetheless, recall that our primary scheduling objective is to minimize SLA violations and our slack time prediction model is devised in accordance with that principle (i.e., overestimate a batched input's execution time for a conservative slack prediction, Equation 2). As such, we propose a profile-driven characterization based approach that sufficiently overprovisions the dynamic DNN's graph-wide estimated latency to minimize the likelihood of SLA violations. The key intuition behind our proposal is that the number of times the dynamic DNN will be unrolled into (i.e., the output sequence length in language translation examples) is determined by *how* the DNN model has been trained. As the training dataset determines how the model gets trained (and accordingly the model's inference time behavior), a detailed characterization across the training dataset can provide a statistical guideline on what is the likelihood of the trained model's recursive layer to be unrolled into a particular output sequence length (i.e., the unrolled decoded sequence number). In other words, the time-unrolled recurrence length will likely fall within the set of output sequence lengths that we observed during the training dataset characterization. Figure 11 summarizes the result of our characterization study which shows what fraction of the training dataset contains sentences with a particular output sequence length. For example, approximately 70% of the English sentences in WMT-2019 training dataset have less than 20 words. Using such profiled information, our proposed approach is to *statically* choose a maximum output sequence length value ($dec_timesteps$ in Algorithm 1) that sufficiently covers more than N-$\%$ of the decoded, output sequence length as observed in the characterization study. For instance, approximately 90% of the translated German sentence word count will likely fall within 30 words, so having the $dec_timesteps$ value be statically set as 30 words (i.e., assume N=90%) will allow the scheduler to conservatively estimate the graph-wide latency (line 8-9 in Algorithm 1). If the output sequence length were to be evaluated smaller than $dec_timesteps$ at runtime (e.g., less than 10 words in the translated German sentence), then the $GraphLatency$ is overly estimated which eventually reduces the estimated slack time. Such conservative estimation of slack time however helps minimize SLA violations, which is our first and foremost scheduling objective. The default configuration of LazyBatching is to set N=90% but service providers can use the value of N, and accordingly the $dec_timesteps$ value, as a tuning knob to balance SLA violations and throughput. In Section VI-C, we quantitatively discuss the sensitivity of LazyBatching to $dec_timesteps$ and demonstrate the robustness of our prediction model.

TABLE I: NPU simulator configuration.

Processor architecture	
Systolic-array dimension	128×128
Operating frequency	700 MHz
On-chip SRAM size (activations & weights)	8 & 4 MB
Memory subsystem	
Number of memory channels	8
Memory access latency	100 cycles
Memory bandwidth	360 GB/sec

D. Putting Everything Together

Overall, our SLA-aware slack time predictor (Equation 2) utilizes domain-specific properties of ML inference (Algorithm 1) for a conservative estimation of slack time, only authorizing batching when the likelihood of an SLA violation is low. The LazyBatching scheduler then utilizes the software-level `BatchTable` as a lightweight control mechanism (Figure 10) for node-level scheduling and batching of active/pending inputs. Compared to baseline graph batching, our proposal can flexibly adapt the level of batching per server inference queries and achieve high system throughput while significantly reducing the number of SLA violations.

V. Methodology

As discussed in Section II-D, our study assumes NPUs as the baseline architecture Due to the lack of publicly accessible NPUs, we resort to a simulation based evaluation methodology in our default settings. The applicability and effectiveness of LazyBatching over real GPU-based inference systems is quantitatively demonstrated later in Section VI-C).

Simulation methodology. The baseline NPU architecture is modeled after Google's TPU design, which employs a systolic-array based microarchitecture [27], [40]. We designed our cycle-level performance model based on [40] as well as public patents from Google [68]–[71]. The performance model has been cross-validated against Google Cloud TPU [29] and SCALE-Sim [73], an open-sourced systolic-array based NPU simulator. Because the compute and memory access characteristics of DNNs exhibit a deterministic dataflow with high data locality, the system-level performance is less sensitive to the complex behavior of the DRAM microarchitecture (e.g., row open/close, refresh, ...). Following prior work [2], [41], [62], we modeled the memory system as having fixed latency and memory bandwidth to reduce simulation time (Table I).

Benchmarks. We employ the methodology employed in MLPerf cloud inference benchmark suite [54] to generate inference request traces. Concretely, we establish an inference query traffic generator which issues inference requests to the model serving system based on a *Poisson distribution* to emulate a server's query-arrival rates as in other relevant prior work [25], [61], [63], [76]. The parameters of our Poisson distribution are chosen to model the low/medium/heavy load traffic to the inference server (i.e., 0-256/256-500/500+

TABLE II: Evaluated benchmarks.

Network name	Application	ML algorithm	Single-batch latency
ResNet [72]	Vision	CNN	1.1 ms
GNMT [6]	Translation	RNN	7.2 ms
Transformer [79]	Translation	Attentions	2.4 ms

queries/sec for low/medium/heavy traffic), in accordance with the single-input inference latency of our studied workload, which ranges from $1-7$ ms (Table II). In terms of the evaluated benchmarks, the main evaluation section (Section VI-A and Section VI-B) primarily focuses on three workloads summarized in Table II for a detailed analysis of LazyBatching's effectiveness across different dimensions. We select two applications from the MLPerf inference benchmark suite used for computer vision (ResNet) and machine translation (GNMT). We also study an attention-based machine translation application (Transformer) included as part of the MLPerf training benchmark suite, which we utilize for inference. Both GNMT and Transformer assume an English-to-German sentence translation scenario with a maximum sentence length of 80 words. Later in Section VI-C, we quantify the robustness of LazyBatching across a broader set of applications by studying its performance across four additional benchmarks (i.e., VGGNet [77], MobileNet [35], Listen-Attend-and-Spell [7], and BERT [17]) during our sensitivity analysis. To model the *predicted* and *actual* time-unrolled output sequence length of seq2seq models, we take the following measure. For a given single-input inference query, we randomly select an English sentence from the WMT-2019 test dataset (unused as part of the profile-based characterization study which uses the training dataset only). The selected English sentence is translated into its corresponding German sentence, which we utilize to count the number of its words and use it to model the *actual* time-unrolled output sequence at runtime. As discussed in Algorithm 1, the *predicted* output sequence length (i.e., $dec_timesteps$) is fixed at a static threshold value assuming N=90% coverage of our profile-driven characterization study (Figure 11, Section IV-C). The sensitivity of LazyBatching to other translation pairs and alternative $dec_timesteps$ values are discussed in Section VI-C.

VI. Evaluation

We explore four design points in this section: 1) always *serializing* incoming requests without batching (`Serial`), 2) baseline graph batching with a batching time-window of N ms (`GraphB(N)`), 3) our proposed LazyBatching (`LazyB`), and 4) an oracular version of LazyBatching (`Oracle`) that utilizes the precise latency-vs-throughput tradeoff curves (for all possible batch sizes for every node within a target DNN) to estimate SLA slack time and perform lazy batching. For clarity of explanation, graph batching is configured with a model-allowed maximum batch size of 64 as default, but we discuss the sensitivity of our results against other maximum batch sizes in Section VI-C. As SLA target numbers are vendor-specific values not publicly disclosed, we assume the SLA deadline is set to 100 ms for LazyBatching's slack estimation in Section VI-A. The effectiveness of LazyBatching under different SLA targets is discussed in Section VI-B.

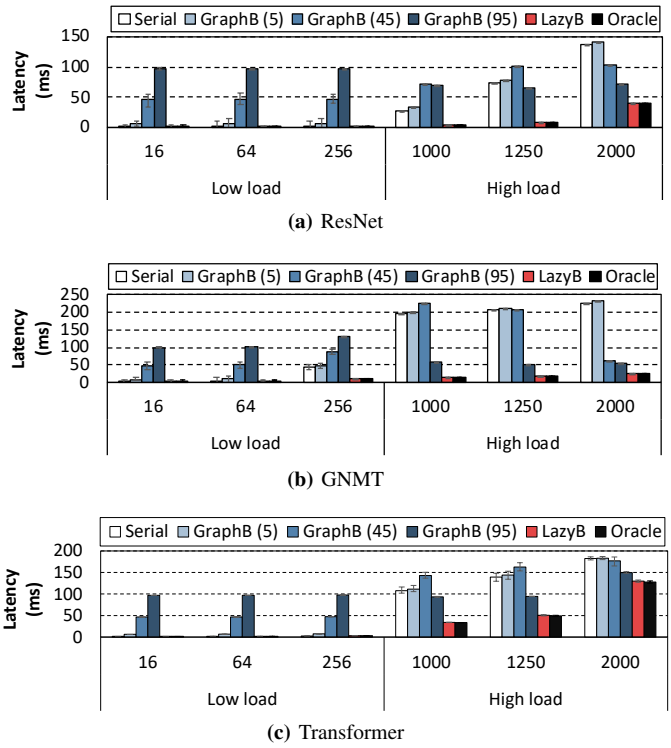

(a) ResNet

(b) GNMT

(c) Transformer

Fig. 12: Effect on average latency per query-arrival rate (x-axis, requests/sec).

We omit the results of cellular batching because none of the workloads we study are solely based on RNN layers, rendering *cellular batching to perform identically to graph batching*. This section reports the averaged results across 20 simulation runs.

A. Effect on Latency and Throughput

Figure 12 and Figure 13 summarize the effect of different batching policies on average latency and throughput per inference query-arrival rate (low vs. high traffic). The error bars represent the 25-percentile and 75-percentile average latency and throughput across difference simulation runs. Under low load server traffic conditions, graph batching consistently performs poorly in terms of both latency and throughput. This is expected as graph batching needlessly stalls inputs from execution, despite having little batching opportunities under low load (especially for large batching time-window configurations such as `GraphB(95)`). Consequently, graph batching experiences significantly longer average latency even compared to `Serial`, which spends much less time waiting to be issued for execution when the server is lightly loaded. For high loads, graph batching performs better than `Serial` as it can amortize the cost of batch collection latency and enhance throughput. Nonetheless, the statically configured batching time-window fails to balance latency and throughput and no single graph batching configuration performs robustly across all applications or server loads.

Our LazyBatching perform superior than both `Serial` and all graph batching configurations as it can adaptively adjust to different query-arrival rates, minimizing the latency in forming batched inputs while still reaping out the benefits

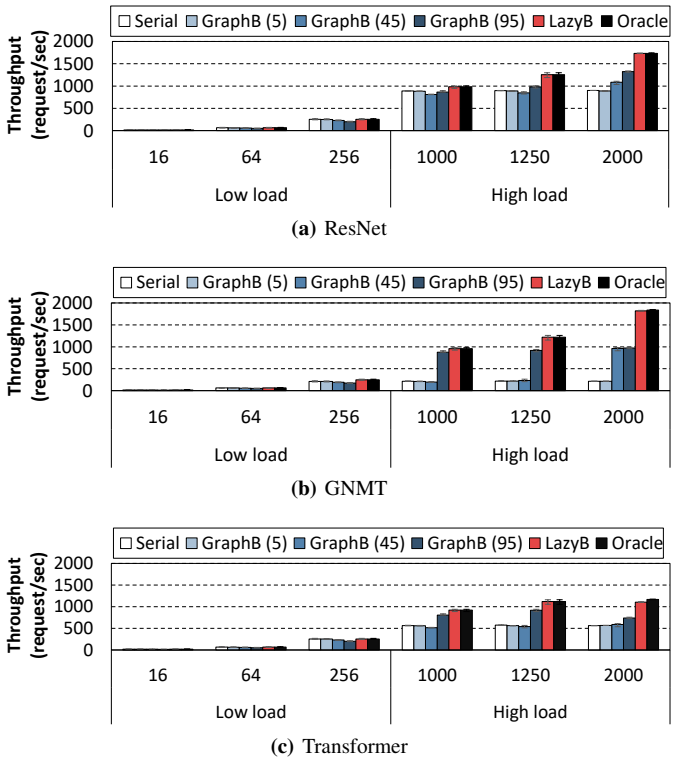

(a) ResNet

(b) GNMT

(c) Transformer

Fig. 13: Effect on throughput per query-arrival rate (x-axis, requests/sec).

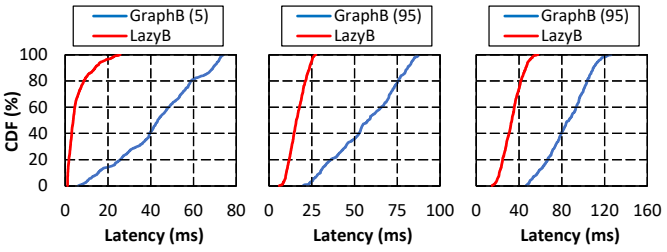

(a) ResNet (b) GNMT (c) Transformer

Fig. 14: CDF of inference latency under high load (1K req/sec), showing LazyBatching's effectiveness in reducing *tail latency*. For clarity, we only plot the best performing graph batching configuration for each workload.

of batching for improved throughput. Overall, LazyBatching provides 5.3×, 2.7×, and 2.5× lower latency than the best performing graph batching for ResNet, GNMT, and Transformer, respectively. At the same time, LazyBatching provides similar or even better throughput than the throughput-optimized graph batching, achieving an average 1.1×/1.3×/1.2× improvement than the best performing graph batching solution for ResNet/GNMT/Transformer. These results highlight the robustness of our LazyBatching system, which consistently provides low latency while also achieving the throughput benefits of graph batching. We also illustrate LazyBatching's merits using Figure 14, which shows the cumulative density function (CDF) of end-to-end inference latency. Notice how the 99-percentile latency of LazyBatching is consistently much smaller than the best performing graph batching (e.g., 54 vs. 123 ms of 99-percentile latency for Transformer), demonstrating the effectiveness of our SLA-aware slack prediction algorithm in reducing *tail latency*. We now further detail LazyBatching's effectiveness on minimizing SLA violations thereby guaranteeing QoS.

B. Effectiveness in Meeting SLA Goals

LazyBatching's performance is sensitive to the effectiveness of our slack prediction algorithm, which is dependent on the SLA target value specified per each model deployment scenario. Unfortunately, an ML application's SLA deadline target numbers are vendor-specific, proprietary information not readily accessible. To quantify how well our LazyBatching scheduler minimizes SLA violations, we sweep the SLA target value (SLA_{target} in Equation 2) and measure the fraction of SLA violated inference requests as a function of different batching policies. As shown in Figure 15, graph batching experiences severe SLA violations even when the SLA target is set up loosely (e.g., even at SLA target of 100 ms, two-thirds of graph batching configurations experience more than 50% violations). LazyBatching achieves *zero* SLA violations unless the SLA target is set below 20/40/60 ms for ResNet/GNMT/Transformer, demonstrating its robustness and efficiency even under such tight SLA constraints. What is also noteworthy is that LazyBatching is highly competitive even when compared against `Oracle`, which shows the cost-effectiveness of our lightweight slack prediction algorithm.

C. Sensitivity

LazyBatching robustness to other ML applications. Figure 16 summarizes the effect of LazyBatching on (a) reducing latency, (b) improving throughput, and (c) reducing SLA violations, over the four additional benchmarks, VGGNet (VN), MobileNet (MN), Listen-Attend-and-Spell (LAS), and BERT. As depicted, our LazyBatching remains highly robust across a diverse range of applications, achieving an average 1.5×, 1.3×, and 2.9× improvement in latency, throughput, and SLA satisfaction, respectively.

Estimated unrolled sequence length of dynamic DNNs. LazyBatching utilizes the $dec_timesteps$ value for estimating dynamic DNN's graph-wide latency (Algorithm 1). Under our evaluation setting, choosing a small $dec_timesteps$ value leads to an *optimistic* prediction of end-to-end latency, which increases the estimated slack time and eventually the number of SLA violations. For instance, while LazyBatching with $dec_timesteps$=32 timesteps (i.e., our default configuration with N=90% coverage) achieves *zero* SLA violations under an SLA target deadline of 60 ms, having $dec_timesteps$ set to 10 timesteps (N=16% coverage) leads to an average 36% SLA violation for Transformer. Nonetheless, we observe that LazyBatching's performance remains robust as long as $dec_timesteps$ is sufficiently large enough to overprovision graph-wide latency thus reducing estimated slack time.

Model-allowed maximum batch size. Prior sections assumed that graph batching's maximum batch size is set to 64. When graph batching's maximum batch size is changed to 16 and 32, LazyBatching achieved an average 12×/14× latency reduction, and 1.3×/1.3× improved throughput, respectively.

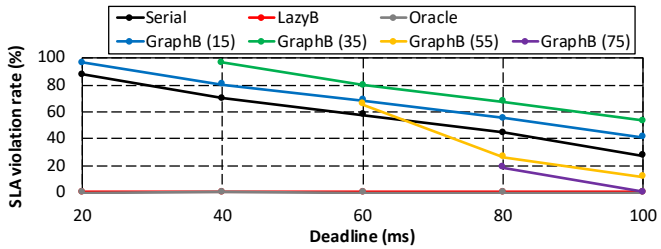

(a) ResNet

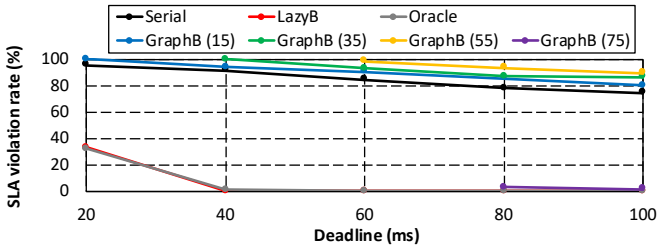

(b) Google Neural Machine Translation (GNMT)

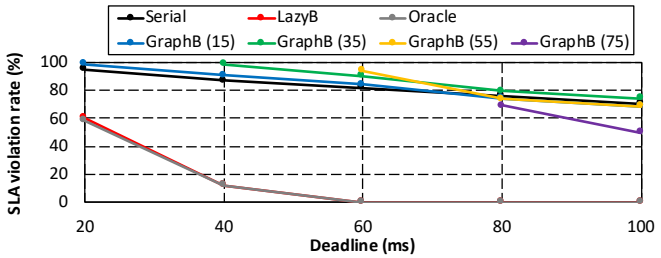

(c) Transformer

Fig. 15: SLA violation rate as a function of batching policy and SLA deadline (x-axis). The query-arrival rate is set to a high load (1K req/sec) to stress test a batching policy's ability to minimize SLA violations (i.e., studying SLA under a low query-arrival rate is meaningless because none will violate the SLA). We omit plotting impractical data points for brevity (e.g., it does not make sense to configure the batching time-window at 75 ms when SLA deadline is 40 ms). As a SLA deadline increases, from left to right in the x-axis, the violation rate monotonically decreases for all policies.

Alternative machine translation scenarios. Our study assumed an English-to-German machine translation pair as our default evaluation setting, but the effectiveness of LazyBatching remains intact for alternative language translation pairs (e.g., Russian-to-English, English-to-French, ...).

LazyBatching for GPU-based inference systems. This subsection so far assumed an NPU-based inference system. We now discuss the applicability and robustness of LazyBatching for GPU-based inference systems. We designed a proof-of-concept software prototype that is implemented on top of NVIDIA CUDA 10.1 and cuDNN 7.0. Our software framework models both the baseline graph batching and our proposed LazyBatching system and the experiments are conducted over an NVIDIA Titan Xp. Compared to graph batching, LazyBatching provides an average $1.4-56\times$ improvement in latency while still achieving competitive system throughput. In terms of QoS, LazyBatching reduces the number of SLA violations by $1.3\times$ (Figure 17). Overall, LazyBatching shows robustness to GPU-based systems.

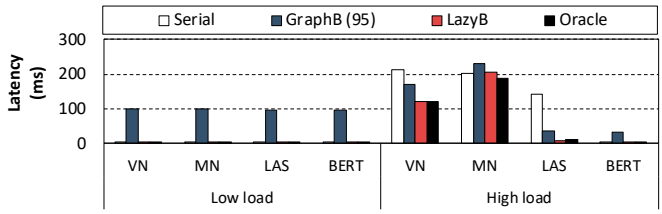

(a) Latency

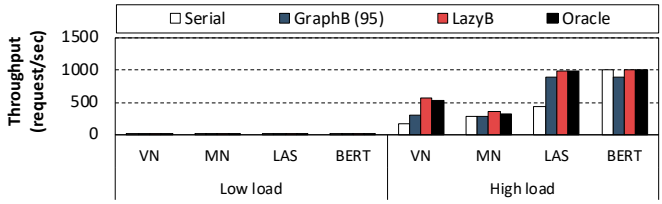

(b) Throughput

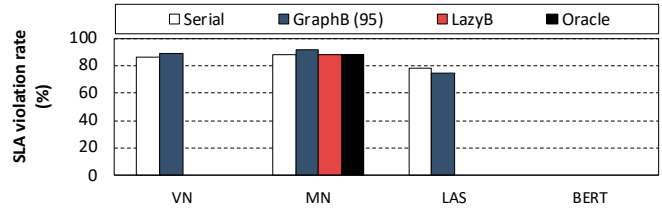

(c) SLA violation rate

Fig. 16: LazyBatching sensitivity to other benchmarks. Due to space constraints, we only show two datapoints under the low/high load in (a,b), assuming 16/1000 requests/sec, respectively. Similarly, the SLA violation rate in (c) summarizes our evaluation under high load (1000 requests/sec) where we report the average violation rate as a single result when sweeping the SLA deadline from 20 to 100 ms. BERT's short end-to-end latency renders the assumed 20-100 ms SLA deadline to not cause any SLA violations even under `Serial`. Regardless, LazyBatching significantly improves latency and throughput under this workload.

LazyBatching for "co-located' ML model inference. Co-locating multiple models within a ML inference server helps improve the server's overall utilization and therefore its total-cost-of-ownership. To clearly separate out the benefits of LazyBatching from the advantages coming from co-location, we have so far assumed that a single model is deployed within the server. To quantify the efficacy of LazyBatching under model co-location, we follow the methodology employed by Choi et al. [14] to implement a model inference server supporting model co-location. Incorporating LazyBatching under co-located ML inference server is straightforward. Whenever a new request is received, our scheduler examines whether lazily batching this request will violate the SLA of the currently on-going requests of co-located ML models, which is used to determine batchability. We implement our proposal and confirm that LazyBatching provides an average $2.4\times/1.8\times$ improvement in latency and throughput than baseline graph batching when when four models are co-located.

D. Implementation Overhead

As detailed in Section IV, LazyBatching is based on the node-level DNN execution model, a property existing ML frameworks and runtime libraries are already founded upon.

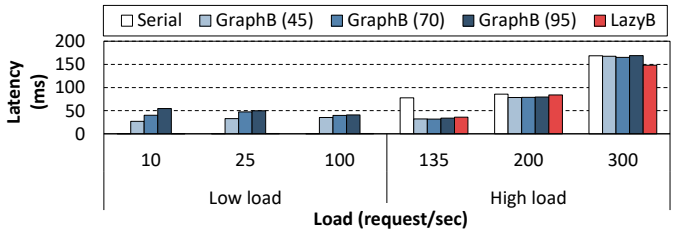

(a) Latency

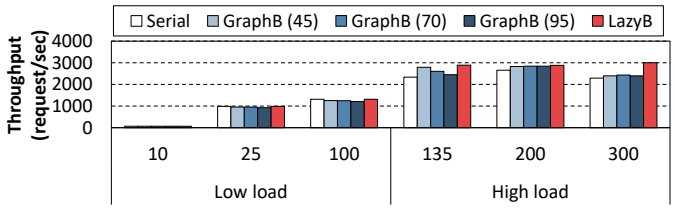

(b) Throughput

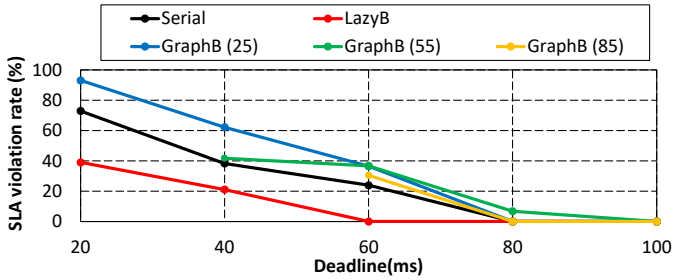

(c) SLA violation rate

Fig. 17: LazyBatching sensitivity to GPU-based inference systems. Due to space constraints, we only present detailed results for Transformer, assuming the same evaluation methodology in Section VI-A and Section VI-B.

As the stack based batch status tracking process is purely done in software and the task preemption and context switching is conducted in node execution boundaries (i.e., layer boundaries), there is no hardware modifications required to implement LazyBatching. As LazyBatching chooses the node at the top of the stack (i.e., batch state table) for scheduling, the scheduling computational complexity is `O(1)` and is thus negligible. In terms of memory allocations for batched requests, the required input/output tensors are allocated upfront to be large enough to accommodate the model-allowed maximum batch size, which amortizes the runtime memory management overhead. Such design decision helps remove the memory allocation latency from the critical path for model inference, a key reason why existing ML inference serving frameworks implement such memory allocation scheme for inference servers. As LazyBatching preempts an on-going batch at the end of a layer's execution, the output activations are stored into DRAM, obviating the need for checkpointing intermediate data. As such, the latency overhead of preemption itself is negligible under LazyBatching. While we were not able to implement our software prototype on top of a real NPU hardware (due to limited availability of NPUs with customizable software frameworks), we confirm through our software GPU prototype implementation that LazyBatching can readily be implemented on top of existing hardware/software stack.

VII. Related Work

While there has been lots of interest in designing energy-efficient NPU architectures for training and inference in isolation [1], [2], [8], [10]–[13], [16], [18], [19], [24], [32], [37], [38], [40], [41], [43]–[51], [55], [56], [58], [62], [65]–[67], [74], [75], [80]–[82], [85], little attention has been paid in *how* the ML inference server collects the batched inputs to feed it into the NPUs. A few recent literature advocates the need for optimizing the batching system in ML. GrandSLAm [42] explores dynamic batching for ML application constructed using *microservices* [3]. However, unlike LazyBatching's fine-grained, layer-wise batching, GrandSLAm conducts batching at the microservice routine granularity, similar to the coarse-grained, baseline graph-level batching. PipeDream [57] exploits *batch-level parallelism* of training to propose an inter-batch, pipelined execution among multiple GPUs. PipeDream's partitioned, inter-batch execution of different layers bears some similarity to layer-wise execution of LazyBatching, but the scope of this work and the proposed solution drastically differ against LazyBatching. The closest to our work is cellular batching [25], which we compare and contrast in Section III-B (recall that cellular batching performs identically to baseline under our workloads). Overall, the key contributions and insights delivered with LazyBatching is orthogonal to the aforementioned prior studies.

VIII. Conclusion

While enabling high throughput is a primary design objective in ML training systems, making sure that the end-user experiences low latency with high QoS is a fundamental requirement for cloud ML inference. This paper introduces LazyBatching, an intelligent batching system that dynamically adjusts the level of batching to meet latency, throughput, and SLA requirements. Compared to the baseline graph batching, LazyBatching provides an average $15\times$, $1.5\times$, $5.5\times$ improvements in terms of user-responsiveness, throughput, and SLA satisfaction, respectively.

References

[1] J. Albericio, A. Delmas, P. Judd, S. Sharify, G. O'Leary, R. Genov, and A. Moshovos, "Bit-pragmatic Deep Neural Network Computing," in *Proceedings of the International Symposium on Microarchitecture (MICRO)*, October 2017.

[2] J. Albericio, P. Judd, T. Hetherington, T. Aamodt, N. E. Jerger, and A. Moshovos, "Cnvlutin: Ineffectual-Neuron-Free Deep Convolutional Neural Network Computing," in *Proceedings of the International Symposium on Computer Architecture (ISCA)*, June 2016.

[3] Amazon, "Amazon AWS Microservices."

[4] ——, "Amazon SageMaker," https://aws.amazon.com/sagemaker/.

[5] D. Amodei, S. Ananthanarayanan, R. Anubhai, J. Bai, E. Battenberg, C. Case, J. Casper, B. Catanzaro, Q. Cheng, G. Chen *et al.*, "Deep Speech 2: End-to-end Speech Recognition in English and Mandarin," in *International conference on machine learning*, 2016, pp. 173–182.

[6] D. Britz, A. Goldie, M.-T. Luong, and Q. Le, "Massive Exploration of Neural Machine Translation Architectures," *arXiv preprint arXiv:1703.03906*, 2017.

[7] W. Chan, N. Jaitly, Q. V. Le, and O. Vinyals, "Listen, Attend, and Spell," *arXiv preprint arXiv:1508.01211*, 2015.

[8] T. Chen, Z. Du, N. Sun, J. Wang, C. Wu, Y. Chen, and O. Temam, "DianNao: A Small-footprint High-throughput Accelerator for Ubiquitous Machine-learning," in *Proceedings of the International Conference on Architectural Support for Programming Languages and Operation Systems (ASPLOS)*, March 2014.

[9] T. Chen, M. Li, Y. Li, M. Lin, N. Wang, M. Wang, T. Xiao, B. Xu, C. Zhang, and Z. Zhang, "MXNet: A Flexible and Efficient Machine Learning Library for Heterogeneous Distributed Systems," in *Proceedings of the Workshop on Machine Learning Systems*, December 2015.

[10] Y. Chen, T. Krishna, J. Emer, and V. Sze, "Eyeriss: An Energy-Efficient Reconfigurable Accelerator for Deep Convolutional Neural Networks," in *Proceedings of the International Solid State Circuits Conference (ISSCC)*, February 2016.

[11] Y. Chen, T. Luo, S. Liu, S. Zhang, L. He, J. Wang, L. Li, T. Chen, Z. Xu, N. Sun, and O. Temam, "DaDianNao: A Machine-Learning Supercomputer," in *Proceedings of the International Symposium on Microarchitecture (MICRO)*, December 2014.

[12] P. Chi, S. Li, C. Xu, T. Zhang, J. Zhao, Y. Liu, Y. Wang, and Y. Xie, "A Novel Processing-in-memory Architecture for Neural Network Computation in ReRAM-based Main Memory," in *Proceedings of the International Symposium on Computer Architecture (ISCA)*, June 2016.

[13] Y. Choi and M. Rhu, "PREMA: A Predictive Multi-task Scheduling Algorithm For Preemptible Neural Processing Units," in *Proceedings of the International Symposium on High-Performance Computer Architecture (HPCA)*, 2020.

[14] ——, "PREMA: A Predictive Multi-task Scheduling Algorithm For Preemptible Neural Processing Units," in *Proceedings of the International Symposium on High-Performance Computer Architecture (HPCA)*, 2020.

[15] J. Chung, C. Gulcehre, K. Cho, and Y. Bengio, "Gated Feedback Recurrent Neural Networks," in *International conference on machine learning*, 2015, pp. 2067–2075.

[16] A. Delmas, P. Judd, D. M. Stuart, Z. Poulos, M. Mahmoud, S. Sharify, M. Nikolic, and A. Moshovos, "Bit-tactical: Exploiting Ineffectual Computations in Convolutional Neural Networks: Which, Why, and How," *arXiv preprint arXiv:1803.03688*, 2018.

[17] J. Devlin, M.-W. Chang, K. Lee, and K. Toutanova, "BERT: Pre-training of Deep Bidirectional Transformers for Language Understanding," *arXiv preprint arXiv:1810.04805*, 2018.

[18] Z. Du, R. Fasthuber, T. Chen, P. Ienne, L. Li, T. Luo, X. Feng, Y. Chen, and O. Temam, "ShiDianNao: Shifting Vision Processing Closer to the Sensor," in *Proceedings of the International Symposium on Computer Architecture (ISCA)*, June 2015.

[19] Z. Du, D. Rubin, Y. Chen, L. He, T. Chen, L. Zhang, C. Wu, and O. Temam, "Neuromorphic Accelerators: A Comparison Between Neuroscience and Machine-Learning Approaches," in *Proceedings of the International Symposium on Microarchitecture (MICRO)*, December 2015.

[20] A. E. Eshratifar, M. S. Abrishami, and M. Pedram, "JointDNN: An Efficient Training and Inference Engine for Intelligent Mobile Cloud Computing Services," *IEEE Transactions on Mobile Computing*, 2019.

[21] Facebook, "PyTorch," https://www.tensorflow.org/.

[22] ——, "Accelerating Facebook's Infrastructure with Application-specific Hardware," 2019.

[23] J. Fowers, K. Ovtcharov, M. Papmichael, T. Massengill, M. Liu, D. Lo, S. Alkalay, M. Haselman, L. Adams, M. Ghandi, S. Heil, P. Patel, A. Sapek, G. Weisz, L. Woods, S. Lanka, S. K. Reienhardt, A. M. Caulfield, E. S. Chung, and D. Burger, "A Configurable Cloud-Scale DNN Processor for Real-Time AI," in *Proceedings of the International Symposium on Computer Architecture (ISCA)*, 2018.

[24] M. Gao, J. Pu, X. Yang, M. Horowitz, and C. Kozyrakis, "TETRIS: Scalable and Efficient Neural Network Acceleration with 3D Memory," in *Proceedings of the International Conference on Architectural Support for Programming Languages and Operation Systems (ASPLOS)*, 2017.

[25] P. Gao, L. Yu, Y. Wu, and J. Li, "Low Latency RNN Inference with Cellular Batching," in *Proceedings of the Thirteenth EuroSys Conference*. ACM, 2018, p. 31.

[26] Google, "TensorFlow," https://www.tensorflow.org/.

[27] Google, "Cloud TPUs: ML accelerators for TensorFlow," 2017.

[28] ——, "Cloud Machine Learning Engine," https://cloud.google.com/ml-engine, 2018.

[29] ——, "Cloud TPU," https://cloud.google.com/tpu, 2018.

[30] ——, "TensorFlow Serving for Model Deployment in Production," 2018.

[31] Habana, "Habana Gaudi and Goya: New Levels of AI Performance, Low Power and Cost Efficiency for Datacenter & Cloud," https://habana.ai/.

[32] S. Han, X. Liu, H. Mao, J. Pu, A. Pedram, M. Horowitz, and W. Dally, "EIE: Efficient Inference Engine on Compressed Deep Neural Network," in *Proceedings of the International Symposium on Computer Architecture (ISCA)*, June 2016.

[33] K. Hazelwood, S. Bird, D. Brooks, S. Chintala, U. Diril, D. Dzhulgakov, M. Fawzy, B. Jia, Y. Jia, A. Kalro, J. Law, K. Lee, J. Lu, P. Noordhuis, M. Smelyanskiy, L. Xiong, and X. Wang, "Applied Machine Learning at Facebook: A Datacenter Infrastructure Perspective," in *Proceedings of the International Symposium on High-Performance Computer Architecture (HPCA)*, 2018.

[34] S. Hochreiter and J. Schmidhuber, "Long Short Term Memory," *Neural Computation*, vol. 9, no. 9, pp. 1735–1780, November 1997.

[35] A. G. Howard, M. Zhu, B. Chen, D. Kalenichenko, W. Wang, T. Weyand, M. Andreetto, and H. Adam, "Mobilenets: Efficient Convolutional Neural Networks for Mobile Vision Applications," *arXiv preprint arXiv:1704.04861*, 2017.

[36] HPCWire, "AI Cloud Competition Heats Up: Google's TPU, Amazon Building AI Chip," 2018.

[37] R. Hwang, T. Kim, Y. Kwon, and M. Rhu, "Centaur: A Chiplet-based, Hybrid Sparse-Dense Accelerator for Personalized Recommendations," in *Proceedings of the International Symposium on Computer Architecture (ISCA)*, 2020.

[38] B. Hyun, Y. Kwon, Y. Choi, J. Kim, and M. Rhu, "NeuMMU: Architectural Support for Efficient Address Translations in Neural Processing Units," in *Proceedings of the International Conference on Architectural Support for Programming Languages and Operation Systems (ASPLOS)*, 2020.

[39] Z. Jia, M. Zaharia, and A. Aiken, "Beyond Data and Model Parallelism for Deep Neural Networks," *arXiv preprint arXiv:1807.05358*, 2018.

[40] N. P. Jouppi, C. Young, N. Patil, D. Patterson, G. Agrawal, R. Bajwa, S. Bates, S. Bhatia, N. Boden, A. Borchers, R. Boyle, P. Cantin, C. Chao, C. Clark, J. Coriell, M. Daley, M. Dau, J. Dean, B. Gelb, T. V. Ghaemmaghami, R. Gottipati, W. Gulland, R. Hagmann, C. R. Ho, D. Hogberg, J. Hu, R. Hundt, D. Hurt, J. Ibarz, A. Jaffey, A. Jaworski, A. Kaplan, H. Khaitan, D. Killebrew, A. Koch, N. Kumar, S. Lacy, J. Laudon, J. Law, D. Le, C. Leary, Z. Liu, K. Lucke, A. Lundin, G. MacKean, A. Maggiore, M. Mahony, K. Miller, R. Nagarajan, R. Narayanaswami, R. Ni, K. Nix, T. Norrie, M. Omernick, N. Penukonda, A. Phelps, J. Ross, M. Ross, A. Salek, E. Samadiani, C. Severn, G. Sizikov, M. Snelham, J. Souter, D. Steinberg, A. Swing, M. Tan, G. Thorson, B. Tian, H. Toma, E. Tuttle, V. Vasudevan, R. Walter, W. Wang, E. Wilcox, and D. H. Yoon, "In-datacenter Performance Analysis of a Tensor Processing Unit," in *Proceedings of the International Symposium on Computer Architecture (ISCA)*, June 2017.

[41] P. Judd, J. Albericio, T. Hetherington, T. Aamodt, and A. Moshovos, "Stripes: Bit-serial Deep Neural Network Computing," in *Proceedings of the International Symposium on Microarchitecture (MICRO)*, October 2016.

[42] R. S. Kannan, L. Subramanian, A. Raju, J. Ahn, J. Mars, and L. Tang, "GrandSLAm: Guaranteeing SLAs for Jobs in Microservices Execution Frameworks," in *Proceedings of the Fourteenth EuroSys Conference 2019*, 2019, pp. 1–16.

[43] D. Kim, J. Kung, S. Chai, S. Yalamanchili, and S. Mukhopadhyay, "Neurocube: A Programmable Digital Neuromorphic Architecture with High-Density 3D Memory," in *Proceedings of the International Symposium on Computer Architecture (ISCA)*, June 2016.

[44] Y. Kwon and M. Rhu, "A Disaggregated Memory System for Deep Learning," in *IEEE Micro*, 2019.

[45] Y. Kwon, Y. Lee, and M. Rhu, "TensorDIMM: A Practical Near-Memory Processing Architecture for Embeddings and Tensor Operations in Deep Learning," in *Proceedings of the International Symposium on Microarchitecture (MICRO)*, 2019.

[46] Y. Kwon and M. Rhu, "A Case for Memory-Centric HPC System Architecture for Training Deep Neural Networks," in *IEEE Computer Architecture Letters*, 2018.

[47] ——, "Beyond the Memory Wall: A Case for Memory-Centric HPC System for Deep Learning," in *Proceedings of the International Symposium on Microarchitecture (MICRO)*, 2018.

[48] R. LiKamWa, Y. Hou, M. Polansky, Y. Gao, and L. Zhong, "RedEye: Analog ConvNet Image Sensor Architecture for Continuous Mobile Vision," in *Proceedings of the International Symposium on Computer Architecture (ISCA)*, June 2016.

[49] D. Liu, T. Chen, S. Liu, J. Zhou, S. Zhou, O. Temam, X. Feng, X. Zhou, and Y. Chen, "PuDianNao: A Polyvalent Machine Learning Accelerator," in *Proceedings of the International Conference on Architectural Support for Programming Languages and Operation Systems (ASPLOS)*, April 2015.

[50] S. Liu, Z. Du, J. Tao, D. Han, T. Luo, Y. Xie, Y. Chen, and T. Chen, "Cambricon: An Instruction Set Architecture for Neural Networks," in *Proceedings of the International Symposium on Computer Architecture (ISCA)*, 2016.

[51] D. Mahajan, J. Park, E. Amaro, H. Sharma, A. Yazdan-bakhsh, J. Kim, and H. Esmaeilzadeh, "TABLA: A Unified Template-based Framework for Accelerating Statistical Machine Learning," in *Proceedings of the International Symposium on High-Performance Computer Architecture (HPCA)*, February 2016.

[52] Microsoft, "Microsoft Azure Machine Learning Studio," https://studio.azureml.net, 2018.

[53] MIT Technology Review, "Why Facebook Want to Design Its Own AI Chips," 2018.

[54] MLPerf, "MLPerf: A Broad ML Benchmark Suite for Measuring Performance of ML Software Frameworks, ML Hardware Accelerators, and ML Cloud Platforms," https://github.com/mlperf/inference/tree/master/cloud, 2020.

[55] D. Moss, S. Krishnan, E. Nurvitadhi, P. Ratuszniak, C. Johnson, J. Sim, A. Mishra, D. Marr, S. Subhaschandra, and P. Leong, "A Customizable Matrix Multiplication Framework for the Intel HARPv2 Xeon+FPGA Platform: A Deep Learning Case Study," in *Proceedings of the International Symposium on Field-Programmable Gate Arrays (FPGA)*, 2018.

[56] D. Moss, E. Nurvitadhi, J. Sim, A. Mishra, D. Marr, S. Subhaschandra, and P. Leong, "High Performance Binary Neural Networks on the Xeon+FPGA Platform," in *Proceedings of the International Conference on Field Programmable Logic and Applications (FPL)*, 2017.

[57] D. Narayanan, A. Harlap, A. Phanishayee, V. Seshadri, N. R. Devanur, G. R. Ganger, P. B. Gibbons, and M. Zaharia, "PipeDream: Generalized Pipeline Parallelism for DNN Training," in *Proceedings of the 27th ACM Symposium on Operating Systems Principles*, 2019, pp. 1–15.

[58] E. Nurvitadhi, G. Venkatesh, J. Sim, D. Marr, R. Huang, J. Ong, Y. Liew, K. Srivatsan, D. Moss, S. Subhaschandra, and G. Boudoukh, "Can FPGAs Beat GPUs in Accelerating Next-Generation Deep Neural Networks?" in *Proceedings of the International Symposium on Field-Programmable Gate Arrays (FPGA)*, 2017.

[59] NVIDIA, "cuDNN: GPU Accelerated Deep Learning," 2016.

[60] ——, "TensorRT Inference Server User Guide," 2018.

[61] A. Ousterhout, J. Fried, J. Behrens, A. Belay, and H. Balakrishnan, "Shenango: Achieving High CPU Efficiency for Latency-sensitive Datacenter Workloads," in *16th USENIX Symposium on Networked Systems Design and Implementation (NSDI)*, 2019, pp. 361–378.

[62] A. Parashar, M. Rhu, A. Mukkara, A. Puglielli, R. Venkatesan, B. Khailany, J. Emer, S. W. Keckler, and W. J. Dally, "SCNN: An Accelerator for Compressed-sparse Convolutional Neural Networks," in *Proceedings of the International Symposium on Computer Architecture (ISCA)*, June 2017.

[63] Y. Peng, Y. Bao, Y. Chen, C. Wu, and C. Guo, "Optimus: An Efficient Dynamic Resource Scheduler for Deep Learning Clusters," in *Proceedings of the Thirteenth EuroSys Conference*. ACM, 2018, p. 3.

[64] A. Radford, J. Wu, R. Child, D. Luan, D. Amodei, and I. Sutskever, "Language Models Are Unsupervised Multitask Learners," *OpenAI Blog*, vol. 1, no. 8, 2019.

[65] B. Reagen, P. Whatmough, R. Adolf, S. Rama, H. Lee, S. Lee, J. Miguel, H. Lobato, G. Wei, and D. Brooks, "Minerva: Enabling Low-Power, High-Accuracy Deep Neural Network Accelerators," in *Proceedings of the International Symposium on Computer Architecture (ISCA)*, June 2016.

[66] M. Rhu, N. Gimelshein, J. Clemons, A. Zulfiqar, and S. W. Keckler, "vDNN: Virtualized Deep Neural Networks for Scalable, Memory-Efficient Neural Network Design," in *Proceedings of the International Symposium on Microarchitecture (MICRO)*, October 2016.

[67] M. Rhu, M. O'Connor, N. Chatterjee, J. Pool, Y. Kwon, and S. W. Keckler, "Compressing DMA Engine: Leveraging Activation Sparsity for Training Deep Neural Networks," in *Proceedings of the International Symposium on High-Performance Computer Architecture (HPCA)*, February 2018.

[68] J. Ross, "Prefetching Weights for Use in a Neural Network Processor," Patent, 05 2015, uS 9805304B2.

[69] J. Ross, N. Jouppi, A. Phelps, R. Young, T. Norrie, G. Thorson, and D. Luu, "Neural Network Processor," Patent, 05 2015, uS 9747546B2.

[70] J. Ross and A. Phelps, "Computing Convolutions Using a Neural Network Processor," Patent, 05 2015, uS 9697463B2.

[71] J. Ross and G. Thorson, "Rotating Data for Neural Network Computations," Patent, 05 2015, uS 9747548B2.

[72] S. Gross and M. Wilber, "Training and Investigating Residual Nets," 2016.

[73] A. Samajdar, Y. Zhu, P. Whatmough, M. Mattina, and T. Krishna, "Scale-sim: Systolic CNN Accelerator Simulator," *arXiv preprint arXiv:1811.02883*, 2018.

[74] A. Shafiee, A. Nag, N. Muralimanohar, R. Balasubramonian, J. P. Strachan, M. Hu, R. S. Williams, and V. Srikumar, "ISAAC: A Convolutional Neural Network Accelerator with In-Situ Analog Arithmetic in Crossbars," in *Proceedings of the International Symposium on Computer Architecture (ISCA)*, June 2016.

[75] H. Sharma, J. Park, D. Mahajan, E. Amaro, J. Kim, C. Shao, A. Misra, and H. Esmaeilzadeh, "From High-level Deep Neural Models to FPGAs," in *Proceedings of the International Symposium on Microarchitecture (MICRO)*, 2016.

[76] H. Shen, L. Chen, Y. Jin, L. Zhao, B. Kong, M. Philipose, A. Krishnamurthy, and R. Sundaram, "Nexus: A GPU Cluster Engine for Accelerating DNN-based Video Analysis," in *Proceedings of the 27th ACM Symposium on Operating Systems Principles*. ACM, 2019, pp. 322–337.

[77] K. Simonyan and A. Zisserman, "Very Deep Convolutional Networks for Large-Scale Image Recognition," *arXiv preprint arXiv:1409.1556*, 2014.

[78] I. Sutskever, O. Vinyals, and Q. Le, "Sequence to Sequence Learning with Neural Networks," in *Proceedings of the International Conference on Neural Information Processing Systems (NIPS)*, 2014.

[79] A. Vaswani, N. Shazeer, N. Parmar, J. Uszkoreit, L. Jones, A. N. Gomez, Ł. Kaiser, and I. Polosukhin, "Attention Is All You Need," in *Advances in neural information processing systems*, 2017, pp. 5998–6008.

[80] G. Venkatesh, E. Nurvitadhi, and D. Marr, "Accelerating Deep Convolutional Networks Using Low-precision and Sparsity," in *Proceedings of the IEEE International Conference on Acoustics, Speech and Signal Processing (ICASSP)*, 2017.

[81] P. Whatmough, S. Lee, H. Lee, S. Rama, D. Brooks, and G. Wei, "A 28nm SoC with a 1.2 GHz 568nJ/Prediction Sparse Deep-Neural-Network Engine with $>$0.1 Timing Error Rate Tolerance for IoT Applications," in *Proceedings of the International Solid State Circuits Conference (ISSCC)*, February 2017.

[82] P. Whatmough, S. Lee, N. Mulholland, P. Hansen, S. Kodali, D. Brooks, and G. Wei, "DNN ENGINE: A 16nm Sub-uJ Deep Neural Network Inference Accelerator for the Embedded Masses," in *Hot Chips: A Symposium on High Performance Chips*, August 2017.

[83] WMT, "WMT-2019 Evaluation Campaign Training Data, News Crawl:articles," http://www.statmt.org/wmt19/translation-task.html, 2019.

[84] Xilinx, "Versal: The First Adaptive Compute Acceleration Platform (ACAP)," 2018.

[85] S. Zhang, Z. Du, L. Zhang, H. Lan, S. Liu, L. Li, Q. Guo, T. Chen, and Y. Chen, "Cambricon-X: An Accelerator for Sparse Neural Networks," in *Proceedings of the International Symposium on Microarchitecture (MICRO)*, October 2016.